Soil & Tillage Research 177 (2018) 1–11

Contents lists available at ScienceDirect

Soil & Tillage Research

journal homepage: www.elsevier.com/locate/still

Research paper

# Comparison of runoff and soil loss in different tillage systems in the Mollisol region of Northeast China

Ximeng Xu[a], Fenli Zheng[a,b,*], G.V. Wilson[c], Chao He[a], Jia Lu[a], Feng Bian[a]

[a] State Key Laboratory of Soil Erosion and Dryland Farming on the Loess Plateau, Institute of Soil and Water Conservation, Northwest A & F University, Yangling 712100, Shaanxi, PR China
[b] Institute of Soil and Water Conservation, CAS & MWR, Yangling 712100, Shaanxi, PR China
[c] USDA-ARS National Sedimentation Laboratory, Oxford 38655, MS, USA

ARTICLE INFO

*Keywords:*
Contour ridge system
Ridge failure
Overland flow concentration
Conservation tillage
Rainfall simulation

ABSTRACT

Longitudinal ridge tillage is the conventional tillage method in the cold, Mollisol region of Northeast China in which furrows are oriented up and down the slope. In part due to the use of this tillage system with large slope lengths, soil erosion is a serious problem in this region. Currently, it is unclear what the best tillage system and ridge orientation is for sustainable agriculture in this region. Thus to compare the runoff and soil loss in longitudinal (LRS) and contour ridge (CRS) systems to a flat tillage system (FTS), a series of simulated rainfall experiments were conducted. A large soil pan (8 m-long, 1.5 m-wide, and 0.6 m-deep) and a side sprinkler rainfall simulation system were used in this study with the three tillage systems (LRS, CRS, FTS) under three rainfall intensities (50, 75 and 100 mm $h^{-1}$) at a 5° slope gradient. The results showed that runoff and soil loss in the LRS were larger than those in the CRS and FTS due to a shift in erosion pattern from sheet to concentrated flow erosion along furrows which led to shear stress increases. Contour ridge failures occurred in the 75 and 100 mm $h^{-1}$ treatments by breaching of ridges when water stored in furrows exceeded their storage capacity. Breaching changed the runoff and soil loss by providing a large sediment source to the convergent flow. Water storage of CRS furrows was constant as rainfall intensity varied which led to overtopping during large storm conditions. Shifting conventional LRS to CRS with modifications to retain more rainwater during low to moderate rainfall events is highly recommended as this would reduce soil loss and enhance infiltration. The FTS exhibited the lowest runoff and soil loss which is recommended for the Mollisol region of Northeast China in large storm conditions.

## 1. Introduction

Ridge tillage is a popular agronomic practice widely used around the world with many different modifications but with the same goal to prepare a seedbed that is elevated above the natural land surface (Lal, 1990; Gürsoy et al., 2012). Ridge tillage affects soil temperature, compaction and water distribution patterns compared to flat-bed tillage, thus, it can improve seed and seedling environment for crop production by providing a drier and warmer seed bed in the spring due to the drainage effect of furrows (Benjamin et al., 1990; Fausey, 1990; Hatfield et al., 1998; Mert et al., 2006; He et al., 2010). There can also be other benefits from ridge tillage, e.g., enhanced rooting depth, improved pest management, nutrient loss control and erosion control (Lal, 1990; Hatfield et al., 1998; Liu et al., 2014a). However, the degree to which such benefits are realized depends to a large extent upon the tillage orientation and the residue management. Ridges oriented up and down the slope can foster concentrated flow which can significantly increase soil loss, and therefore intensify nutrient losses. In contrast, ridges oriented along the contour may store water in furrows, thereby, increasing infiltration and reducing soil losses (Hagmann, 1996; Shen et al., 2005; Arnhold et al., 2013). For no-till ridge systems in which ridges are formed every few years and residue is maintained on the surface between ridge formation years, crop residue protects the soil surface in the furrows from direct rainfall and slows down convergent flows (Jaynes and Swan, 1999).

In response to the climate (freezing conditions in winter and early spring; high snowmelt runoff rate in spring; rainfall mainly concentrated in summer) and topographic conditions (gentle slopes and long slope lengths), ridge tillage is the conventional tillage method in the Mollisol region of Northeast China (Chen et al., 2011; Zhang et al., 2011). Longitudinal ridge system (LRS) in which ridges are oriented up and down the hillslope, perpendicular to the contour, is the dominant

* Corresponding author at: No. 26, Xi'nong Road, Institute of Soil and Water Conservation, Yangling, Shaanxi 712100, PR China.
*E-mail address:* flzh@ms.iswc.ac.cn (F. Zheng).

https://doi.org/10.1016/j.still.2017.10.005
Received 17 April 2017; Received in revised form 2 October 2017; Accepted 31 October 2017

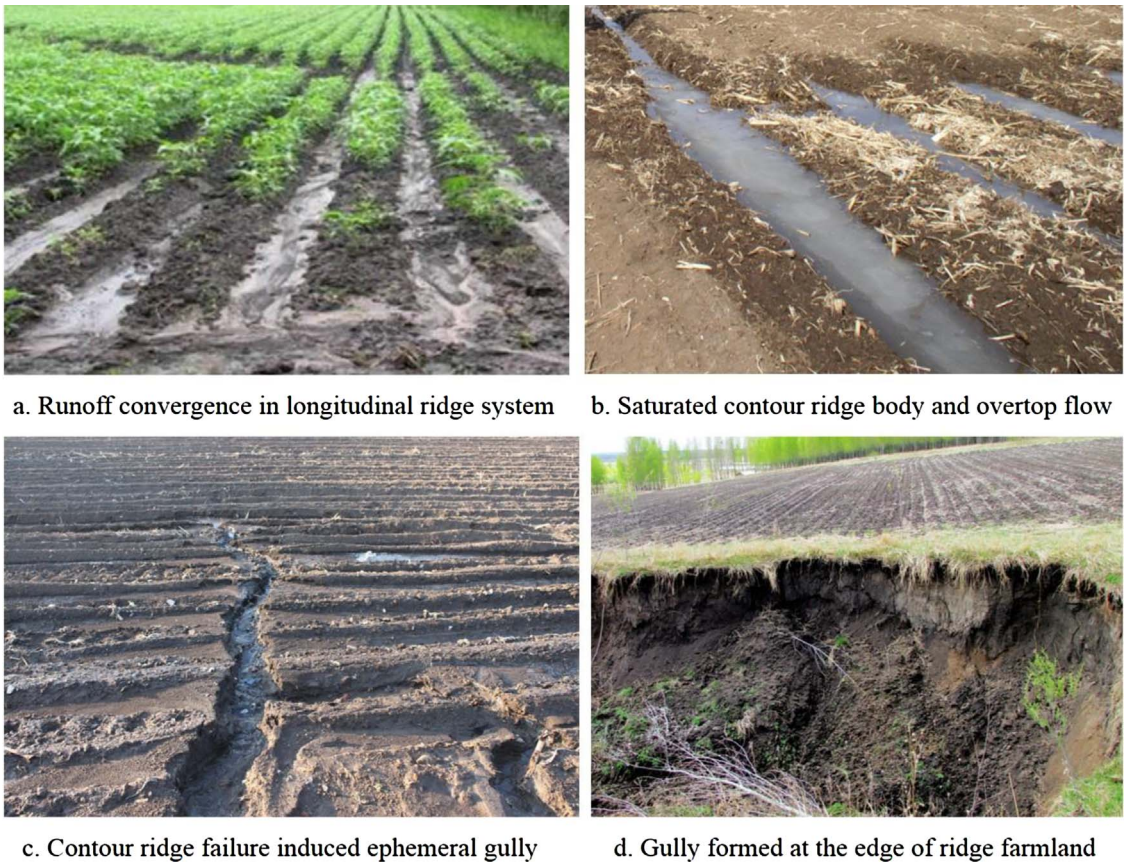


**Fig. 1.** Ridge tillage induced erosion features in the Mollisol region of northeast China.

tillage system in this region (Fig. 1a; Free, 1956; Shen et al., 2005). Contour ridge system (CRS) in which ridges are established along the contour, perpendicular to the overland flow path, is relatively rare in this region. The LRS has long been conceded as accelerating runoff and soil loss in the Mollisol region (Shen et al., 2005; Chen et al., 2008; Meng and Li, 2009), while the CRS is recognized as being more effective in increasing water infiltration (Fig. 1b) and controlling soil erosion than the LRS (Jaynes and Swan, 1999; Shen et al., 2005; Gebreegziabher et al., 2009; Liu et al., 2014a; An et al., 2015).

Contour ridging has been recognized for decades for substantially reducing erosion (Free, 1956; Reeder, 1990; Stevens et al., 2009). However, under extreme rainfall conditions, contour ridges tend to breach and, thereby, foster ephemeral gully erosion (Hatfield et al., 1998; Liu et al., 2014b). Breaching of contour ridges is a concern in Northeast China (Fig. 1c) as erosive storms can occur in the summer with short duration but high intensity and often coincide with snowmelt runoff (Fig. 1b) in spring (Li et al., 2016; Lu et al., 2016). Contour ridge stability is mainly related to ridge geometry, sloping land microtopography, soil physical properties of ridge body, and rainfall characters (Liu et al., 2014b). In RUSLE2, the contouring factor $p_c$ is used to compute the effects of contouring on soil erosion, which is a ratio of erosion with contouring to erosion without contouring, i.e. up and downslope tillage. Experimental data shows that when ridge height is large and slope steepness is small, the contouring subfactor $p_c$ produces relatively small values (USDA-ARS, 2008, 2013). RUSLE2 assumes contouring failure where roughness shear stress computed with Eq. (1) exceeds a critical shear stress which is determined by calibrating critical slope length values given in Agriculture Handbook 537 (Wischmeier and Smith, 1978).

$$\tau_f = q_i^{0.85714} s / n_t^{1.2857} \quad (1)$$

where $\tau_f$ is form roughness shear stress (lbs/ft$^2$); the discharge rate $q_i$ is computed as the product of excess rainfall rate (inches/hour) and the distance along overland flow path (ft); $s$ is overland flow path steepness (%); $n_t$ is total Manning's roughness coefficient (ft$^{1/6}$). However, data are still not sufficient to derive empirical contouring relationships to soil loss in a wide variety of environmental conditions. Thus, further work still needs to be done on the factors influencing soil erosion of the CRS, e.g., suitable ridge geometry for controlling runoff and soil loss, rainfall patterns and microtopography impacts on erosion, etc.

The fertile and productive Mollisols (Black soils) are mainly distributed in a concentrated area in the northeast China with slopes less than 7° but extensive slope lengths that range from 200 to 1000 m (Liu et al., 2011; Li et al., 2016). As a result of the high physical and chemical quality of the native Mollisols, the Mollisol region has been one of the most important grain production bases of China (Meng and Li, 2009; Lu et al., 2016). However, agronomic management over the last 100 years, in combination with high intensity rainfall in summer, snowmelt runoff, and intensive cultivation, has led to the severe runoff and soil loss and wide spread gully erosion (Fig. 1d; Zhang et al., 2007; Liu et al., 2011; An et al., 2012; Lu et al., 2016). According to the soil loss control and ecological security report made by Chinese Ministry of Water Resources and Chinese Academic of Science in 2010, surface mollic thickness was being reduced at a rate of 0.3 to 1 cm per year. The mollic thickness has decreased from 50 to 80 cm in 1950s to 20–40 cm at present as a result of water erosion following reclamation for agriculture use (Zhang et al., 2007). Less productive parent material with low organic matter content is being exposed at the surface in some areas, which greatly decreases the soil quality and reduces crop yield (Yang et al., 2016). Liu et al. (2013) reported that soil depth was the most important indicator of crop yield in the Mollisol region and every 1 cm decrease in depth results in a 2% decrease in yield. Liu and Yan (2009) reported that soil loss and gully erosion on the farmlands in the Mollisol region resulted in a 10.8 billion kg crop yield loss per year.

Thus, erosion is a great threat to agricultural sustainability and food security in this region.

Many researches have characterized the extent of erosion in the Mollisol region of Northeast China (Zhang et al., 2007; An et al., 2012; Lu et al., 2016; Li et al., 2016), but understanding the roles of LRS and CRS compared to flat tillage systems in this region is still lacking. Thus, studies are needed to quantify ridge tillage system impacts on soil erosion in the Mollisol region where sustainable productivity is a national priority but data are scarce.

The objectives of this study were to 1) compare the runoff and soil loss processes in different tillage systems in the Mollisol region of Northeast China; 2) analyze the contour ridge stability and water storage ability; 3) discuss suitable tillage systems for the Mollisol region.

## 2. Material and methods

### 2.1. Experimental setup

#### 2.1.1. Rainfall simulator system

The experiments were conducted in the State Key Laboratory of Soil Erosion and Dryland Farming on the Loess Plateau, Yangling City, China with rainfall and soil properties selected to match field conditions, Table 1. A side sprinkler rainfall simulator system with an adjustable rainfall intensity ranging from 40 to 260 mm $h^{-1}$ was used in the experiments. The system consists of four separate nozzles evenly distributed at two sides above the soil pan (Fig. 2). The fall height of the raindrops was 16 m above the ground which is enough for the most of raindrops to reach terminal velocity. Prior to the experiments, rainfall spatial distribution was tested to make sure that rainfall intensities were evenly distributed over the plot area, and raindrop size calibration was carried out to quantify the match of the simulated raindrop distribution with natural rainfall. Calibration results showed that the spatial uniformity of the simulated rainfall was > 90%. The simulated raindrop diameter distribution was 0.2 to 3.1 mm, and more than 83% of raindrop diameters were < 1.0 mm, which matched the range of field conditions (Table 1).

#### 2.1.2. Soil bed and ridge system

A slope-adjustable, 8-m long, 1.5-m wide and 0.6-m deep soil pan with drainage holes (2 cm aperture) at the bottom was used in this study. The soil pan can be inclined to the slope gradient from 0 to 35° with adjustment steps of 1°. A runoff collecting device was installed on the soil pan outlet, which was used to collect the runoff and sediment samples (Fig. 2).

The tested soil was collected at 0 to 20 cm depth from the plow layer in a maize (*Zea mays* L.) field in Liujia Town (44°43′126°110′E), Yushu City, Jilin Province located at the center of the Mollisol region in Northeast China (Li et al., 2016). The soil used was classified as Mollisol (USDA Taxonomy) with 3.3% sand (> 50 μm), 76.4% silt (50–2 μm), and 20.3% clay (< 2 μm) content. The soil was sieved through a 0.25-mm sieve and organic matters were destroyed before analysis, then pipette method was used to determine the soil texture. The soil organic matter content was 23.8 g $kg^{-1}$ obtained by the potassium dichromate oxidation-external heating method.

Before packing, the soil was air-dried, and then, broken into sub-angular-blocky clods less than 4 cm in size. Impurities such as organic crop residues and gravels were removed. To keep the in-situ soil aggregation fabric, the soil was not sieved and ground.

The soil bed simulated field observations of typical farmlands of the Mollisol region in vertical layering and corresponding bulk densities (Table 1). Soil water content was determined prior to packing to calculate the soil amount needed for packing different soil layers to specific bulk densities in the soil pan. First, the bottom 5 cm of the soil pan were filled with sand to allow free drainage of excess water. A highly permeable cloth was spread on the sand surface to separate the sand layer from the soil layer. Second, a 15-cm plow pan layer with a soil bulk density of 1.35 g $cm^{-3}$ was packed above the sand layer, and a 20-cm tilth layer of Mollisol was packed above the plow pan at a mean bulk density of 1.20 g $cm^{-3}$, which is the average observed surface bulk density value in the Mollisol region. During the packing process, both plow pan and tilth layer were packed in 5-cm increments, and each layer was raked lightly before the next layer was packed to ensure uniformity and continuity in soil structure. Third, different tillage systems were built into the tilth layer. According to field measurements and the size of tillage machines used in Northeast China, the ridge height and width was set as 15 and 65 cm (Chen et al., 2008; Meng and Li, 2009), respectively. For the LRS, two complete furrows and three ridge tops were constructed perpendicular to the contour on the 1.5 m wide soil bed surface, and the length of each ridge was 8 m (Fig. 3a). For the CRS, 12 furrows and 13 ridge tops were constructed parallel to the contour on the 8 m long soil bed surface, and each ridge was 1.5 m long (Fig. 3b). For the FTS, no additional practice was conducted (Fig. 3c). The surface soil bulk density of ridge body was controlled to 1.15–1.25 g $cm^{-3}$, which is the normal range of bulk density after tillage. After building the ridge systems and before rainfall simulation, the soil bed was left untreated for 48 h.

### 2.2. Experimental design

Soil erosion with moderate intensity is generally caused by momentary rainfall intensities larger than 42.6 mm $h^{-1}$, and in some cases, the momentary rainfall intensity can reach 103.2 mm $h^{-1}$ in the typical Mollisol region of Northeast China (Lu et al., 2016). Thus, three rainfall intensities (50, 75, and 100 mm $h^{-1}$) were included in this study. Gentle slope is a basic characteristic of the Mollisol region with slope gradients ranging generally from 3° to 7°. Chen et al. (2008) showed that shifting LRS to CRS at lower slope gradient (< 5°) conditions could obtain great soil conservation effects but small effects when the slope gradient is larger than 5°. Thus, the slope gradient was set to the critical value of 5° to quantify the effects of different ridge systems on soil erosion. Each rainfall experiment lasted 45 min which represented the extreme rainstorm duration observed in the Mollisol region (Table 1). After each rainfall event, soil bed was reconstructed for next experiment run and all treatments were replicated twice on new-built soil beds.

**Table 1**
Comparisons of real field conditions and experimental design.

| Reference factors | Real field condition | Experiment design |
|---|---|---|
| Erosive rainfall intensity (mm $h^{-1}$) | 42.6–103.2 | 50, 75, 100 |
| Raindrop size distribution (mm) | 0.2–3.8 mm, more than half of raindrops were < 1.2 mm | 0.2–3.1 mm, more than 83% of raindrop diameters were < 1.0 mm |
| Soil bulk density of tilth layer | 1.15–1.25 | 1.20 |
| Soil bulk density of plow pan layer | 1.25–1.45 | 1.35 |
| Slope gradient (°) | 3–7 | 5 |
| Average slope length ($m^2$) | 50–1000 | 8 |
| Ridge height (cm) | 13–18 | 15 |
| Ridge space (cm) | 60–70 | 65 |

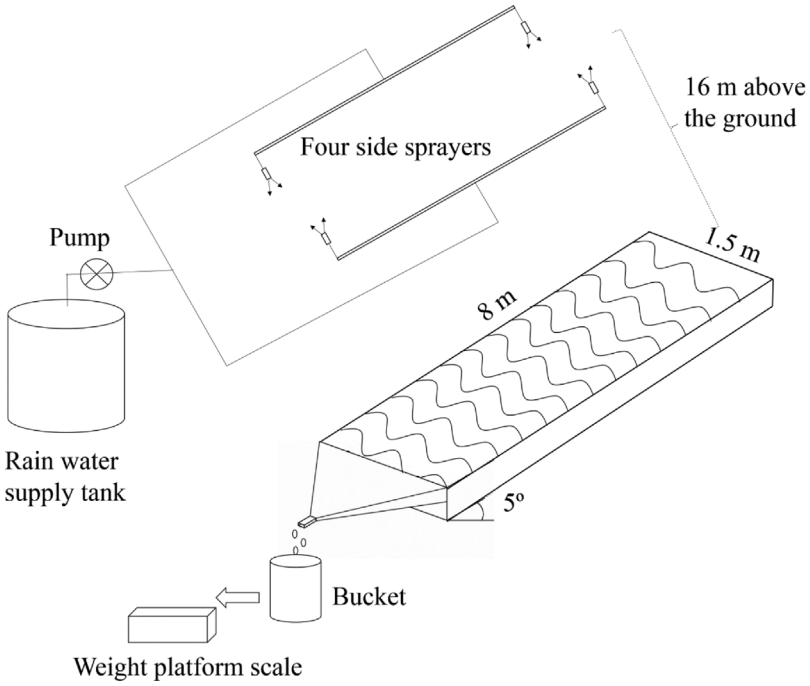


**Fig. 2.** Schematic of the experimental set up.

### 2.3. Experimental procedure

One day before each rainfall event, each treatment had a pre-soak rain applied at 30 mm $h^{-1}$ for around 40 min to the soil surface at a 3° slope gradient until surface runoff occurred. A nylon net with 1 mm aperture was placed 10 cm over the test soil pan prior to the pre-soak to reduce raindrop impacts on surface infiltration (An et al., 2012; Lu et al., 2016). We utilized a pre-soak rainfall to mimic the effect of snow melt in the spring and rainfall in summer that serve to saturate topsoils. The pre-soaking rain was also to ensure comparative uniformity of the surface soil moisture and roughness condition among treatments. A plastic sheet was used to cover the soil bed after pre-soak to prevent evaporation and allow the soil water to equilibrate with depth prior to the experimental runs.

Prior to each rainfall event, calibration of rainfall intensity was conducted to reach the target rainfall intensity and uniformity (> 90%). During each rainfall event, once runoff occurred, runoff and sediment samples were taken consecutively at the soil pan outlet for the first 1 or 2 min and then adapted stepwise to 2-min intervals when the discharge reached steady state. During the rainfall events, surface flow velocities ($V_s$) were measured by using the $KMnO_4$ color tracing method. Flow depth was measured perpendicular to the surface using a thin ruler with 1 mm precision.

The runoff/sediment collection containers used in this experiment were 15-l buckets and the samples were weighed with a platform scale. After sufficient time for sediment settling, the clear supernatant was decanted and all sediment samples were dried in an oven at 105 °C for 48 h. Then the sediment weights were recorded to calculate the runoff rate and sediment yield.

### 2.4. Data analysis

Mean flow velocity was calculated as

$$V = kV_s \quad (2)$$

where $V_s$ (m $s^{-1}$) is the surface flow velocity measured using the dye method, $V$ is the mean flow velocity (m $s^{-1}$), and $k$ is a coefficient taken to be 0.75 (Li et al., 2016).

Shear stress is an important factor for runoff energies to deliver the mass in runoff and was calculated as (Nearing et al., 1991):

$$\tau = \gamma RJ \quad (3)$$

where $\tau$ is shear stress (Pa); $\gamma$ is the weight density of water (N $m^{-3}$); $R$ is hydraulic radius (cm); $J$ is surface slope (m $m^{-1}$) calculated as the


**Fig. 3.** Different tillage systems. Notice that photos of LRS and FTS (a and c) are taken after rainfall test to show the erosion morphology while photo of CRS (b) was taken before test.

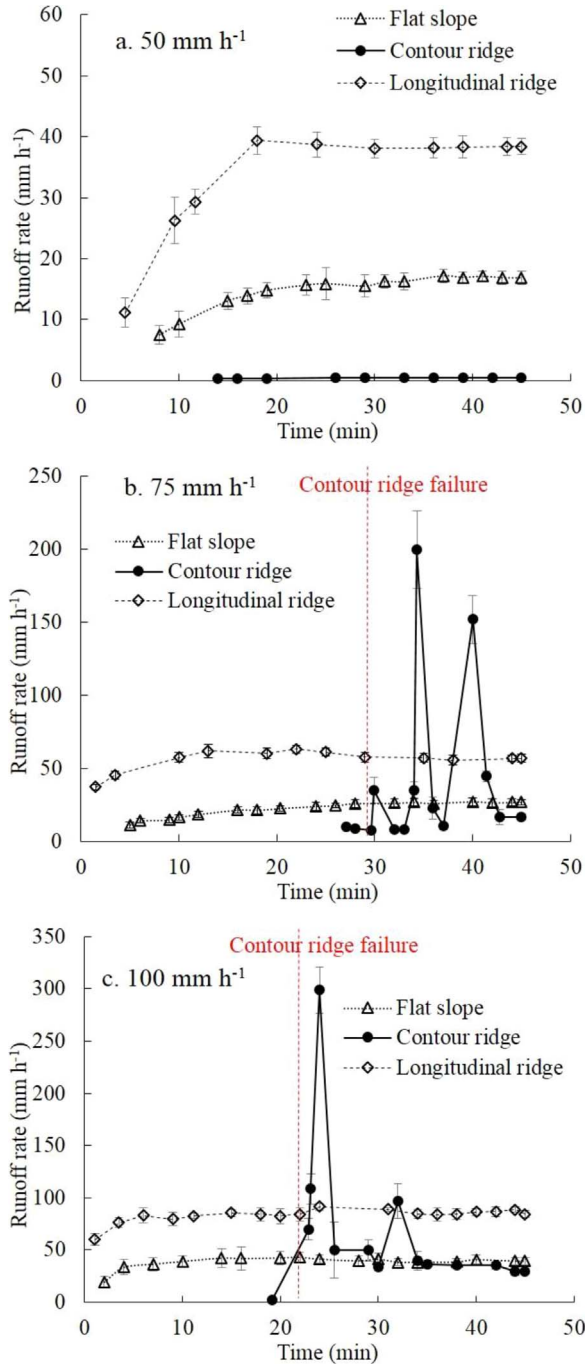


**Fig. 4.** Runoff rate versus run time for different tillage systems. Error bars show the standard deviations of two replicates.

tangent of the slope degree.

## 3. Results

### 3.1. Runoff and soil loss responses

#### 3.1.1. Runoff rates

In the 50 mm $h^{-1}$ treatment, runoff rate for the LRS and FTS exhibited two stages involving an increasing runoff rate stage and a relatively stable stage after 15–20 min (Fig. 4). Runoff for the CRS was minimal as storage capacity of the furrows was not exceeded and, thus, the CRS did not exhibit these stages. Runoff rate stabilized at around 17 mm $h^{-1}$ for the FTS which indicated that 66% of rainfall was infiltrating. In contrast, the runoff rate was around 38 mm $h^{-1}$ for the LRS with only 24% of rainfall infiltrating during this stage. Thus, the stable runoff rate of the LRS was approximately 2.3 times larger than that of the FTS. Given that the runoff rate of the CRS was negligible, either all the rainfall was infiltrated or stored in the furrows.

In the 75 and 100 mm $h^{-1}$ treatments, runoff from the LRS also showed a stable stage, but the time to reach stable runoff was shortened to 10 and 5 min, respectively, and the magnitude of the stable runoff rate increased to 60 mm $h^{-1}$ and 80 mm $h^{-1}$, respectively. While the stable runoff rate corresponding to the 75 and 100 mm $h^{-1}$ rainfall intensity increased, the relative infiltration rate remained around 20% of rainfall. This is in contrast to runoff behavior of the FTS under 75 mm $h^{-1}$ rainfall which did not exhibit a clear stable stage but showed a slow, steady increase in runoff with time reaching a maximum runoff rate of around 27 mm $h^{-1}$. The FTS did exhibit a stable stage for the 100 mm $h^{-1}$ rainfall, reaching the peak in similar time as the LRS at around 5 min but with a stable runoff rate of only around 40 mm $h^{-1}$. The infiltration rate for the FTS was 64% and 60% of rainfall for the75 and 100 mm $h^{-1}$, respectively. Thus, it appears that the relative proportion of rainfall that infiltrates is higher under the FTS than LRS and the infiltrating portion decreases with increasing rainfall intensity for both systems, and the stable runoff rate of the LRS was twice that of the FTS because of runoff convergence in furrows governed by ridge topography.

The CRS exhibited much different behavior than the LRS and FTS for the two higher rainfall intensities with no runoff collected for an extended period (almost 30 and 20 min for 75 and 100 mm $h^{-1}$, respectively). For the CRS to exhibit any appreciable runoff requires ponding in the ridge furrows to overtop the ridges. Once the CRS ridges were over-topped and runoff was initiated, the contour ridges quickly failed. Breaching of the contour ridges resulted in multiple peak instantaneous runoff rates that exceeded 200 and 300 mm $h^{-1}$ for the 75 and 100 mm $h^{-1}$ rainfalls, respectively. Between these peaks in runoff, the runoff rates in the CRS were similar to those or slightly less than those in the FTS.

#### 3.1.2. Soil loss processes

Soil loss rates (Fig. 5) showed some similar and some contrasting trends compared to the runoff response (Fig. 4). Instead of increasing to a stable soil loss rate as observed for runoff, soil loss exhibited a rapid rise to a peak followed by a steady decline for the LRS and a decline to a stable soil loss rate for the FTS. In the 50 mm $h^{-1}$ treatment, soil loss rate of the LRS system initially increased from 1 kg $m^{-2}$ $h^{-1}$ to the peak value of 3 kg $m^{-2}$ $h^{-1}$ at around 10 min and then gradually decreased to the initial value by the end of the experimental run. Soil loss rate of the FTS showed a similar trend but with the peak magnitude at 10 min of only around 0.5 kg $m^{-2}$ $h^{-1}$ and stabilizing at around 0.2 kg $m^{-2}$ $h^{-1}$. There was essentially no soil loss in the CRS as runoff was near zero.

In the 75 mm $h^{-1}$ treatment, soil loss peaked at around 12 min with approximately 7 kg $m^{-2}$ $h^{-1}$ followed by a decrease to a stable rate of around 3 kg $m^{-2}$ $h^{-1}$. In contrast, soil loss for the FTS remained stable at small soil loss rates of less than 1 kg $m^{-2}$ $h^{-1}$. In the 100 mm $h^{-1}$ treatments, soil loss rate of the LRS and FTS systems both showed a peak value at around 7 min into the run followed by a gradual decrease. Soil loss rates of the LRS increased from 8 to 12 kg $m^{-2}$ $h^{-1}$ then decreased to 5 kg $m^{-2}$ $h^{-1}$ as compared to an increase from 1 to 3 kg $m^{-2}$ $h^{-1}$ followed by a decrease to around 2 kg $m^{-2}$ $h^{-1}$ for the FTS. These results showed the great impacts of rainfall intensity on soil loss and the importance of the tillage system as soil loss rates of the LRS were several times larger than those in the FTS as a result of convergent runoff along furrows.

Contour ridge failure is clearly seen in the soil loss rates for the 75 mm $h^{-1}$ and 100 mm $h^{-1}$ treatments for the CRS. Once ridges were breached, the soil loss rates of the CRS exhibited two extreme peak values exceeding 25 kg $m^{-2}$ $h^{-1}$ for the 75 mm $h^{-1}$. In the

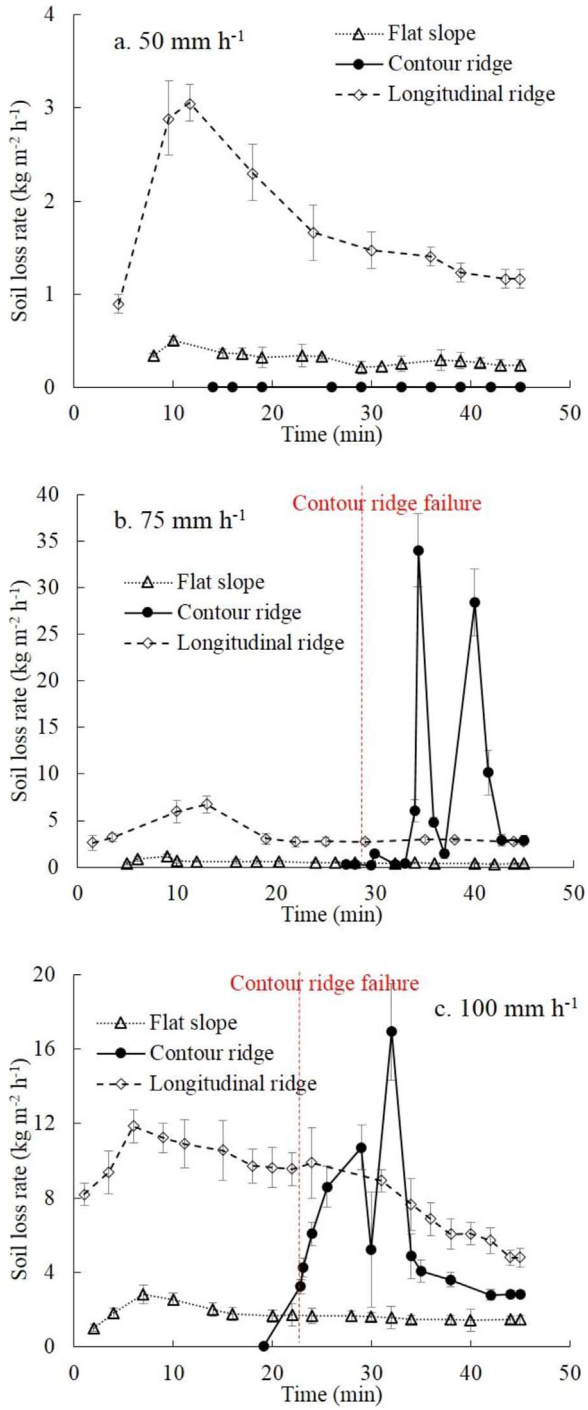


**Fig. 5.** Soil loss rate versus run time for different tillage systems. Error bars show the standard deviations of two replicates.

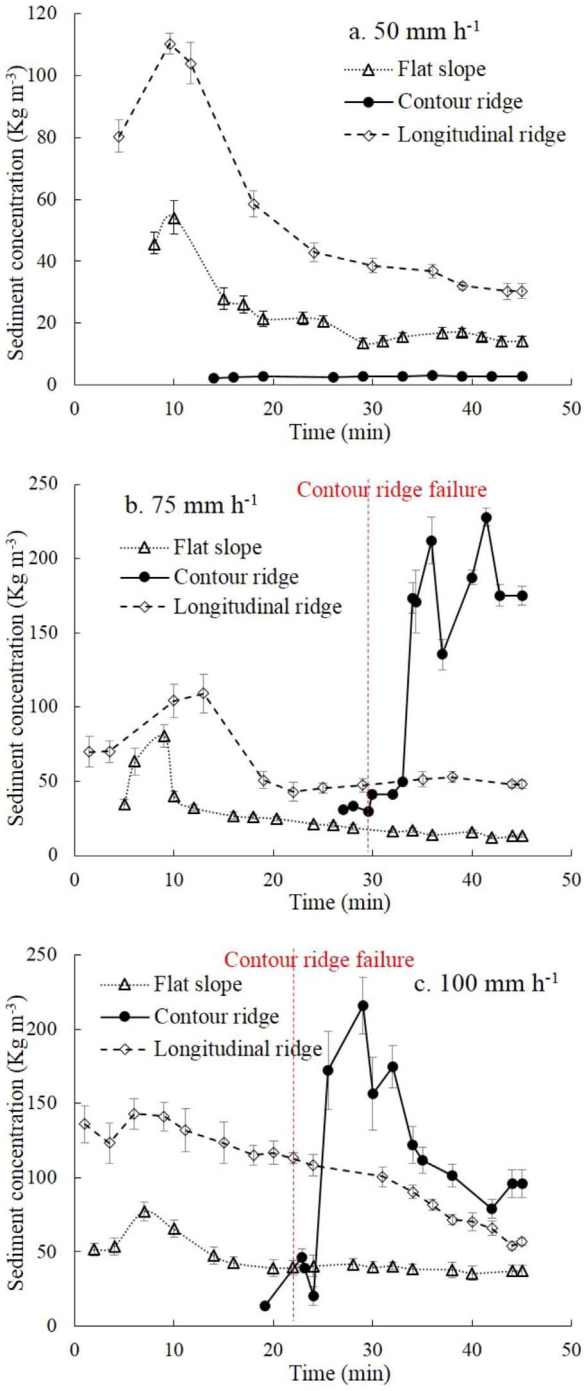


**Fig. 6.** Sediment concentration versus run time for different tillage systems. Error bars show the standard deviations of two replicates.

100 mm $h^{-1}$ treatment, the peak values for the CRS were less than 20 kg $m^{-2}$ $h^{-1}$ but the duration of these peak values were longer. These differences were related to the spatial distribution of the ridge breaching.

### 3.1.3. Sediment concentration processes

The combination of the runoff and soil loss responses is reflected in the sediment concentration variations (Fig. 6). In the 50 mm $h^{-1}$ treatment, sediment concentrations for the different tillage systems were similar to the soil loss trends. Sediment concentration in the LRS and FTS both showed peak values at around 10 min and then decreased with time while sediment concentrations for the CRS were negligible. In the 75 mm $h^{-1}$ treatment, sediment concentrations of the LRS and FTS ranged from 48 to 109 kg $m^{-3}$, and from 12 to 80 kg $m^{-3}$, respectively. Sediment concentration in the CRS after contour ridge failure showed a dramatic rise to about 200 kg $m^{-3}$ but instead of showing a dramatic drop, the concentration remained high with moderate fluctuations until the end of run. In the 100 mm $h^{-1}$ treatment, sediment concentrations of the LRS and FTS ranged from 54 to 143 kg $m^{-3}$, and from 36 to 77 kg $m^{-3}$, respectively. Sediment concentration after contour failure also showed similar dramatic rise to about 200 kg $m^{-3}$ but again remained high with moderate fluctuations comparable to the 75 mm $h^{-1}$ treatment, but a general decrease to about 100 kg $m^{-3}$ by the end of run.

**Table 2**
Runoff and soil loss from each tillage system under different rainfall intensities.

| Rainfall intensity (mm $h^{-1}$) | Tillage system | Total runoff (mm) | Runoff rate (mm $h^{-1}$) | Total soil loss (kg) | Soil loss rate (kg $m^{-2}$ $h^{-1}$) |
|---|---|---|---|---|---|
| 50 | FTS | 8.9 ± 1.3 | 11.9 ± 1.7 | 2.4 ± 0.4 | 0.6 ± 0.1 |
| | LRS | 22.3 ± 3.6 | 29.8 ± 4.8 | 6.4 ± 1.5 | 1.6 ± 0.4 |
| | CRS | 0.2 ± 0.0 | 0.3 ± 0.0 | 0.0 ± 0.0 | 0.0 ± 0.0 |
| 75 | FTS | 15.0 ± 1.4 | 20.0 ± 1.9 | 4.4 ± 0.5 | 1.1 ± 0.1 |
| | LRS | 40.6 ± 2.9 | 54.1 ± 3.9 | 13.7 ± 1.6 | 3.5 ± 0.4 |
| | CRS (before failure) | 0.1 ± 0.0 | 0.3 ± 0.0 | 0.1 ± 0.0 | 0.0 ± 0.0 |
| | CRS (after failure) | 13.3 ± 2.1 | 42.0 ± 6.6 | 25.9 ± 4.3 | 15.8 ± 2.6 |
| 100 | FTS | 27.7 ± 2.8 | 36.9 ± 3.7 | 15.2 ± 1.2 | 3.9 ± 0.3 |
| | LRS | 61.4 ± 6.9 | 81.9 ± 9.2 | 34.7 ± 3.1 | 8.9 ± 0.8 |
| | CRS (before failure) | 0.2 ± 0.0 | 0.6 ± 0.0 | 0.0 ± 0.0 | 0.0 ± 0.0 |
| | CRS (after failure) | 24.5 ± 2.3 | 64.0 ± 6.0 | 27.8 ± 2.9 | 14.0 ± 1.5 |

### 3.2. Total runoff and soil loss

Total runoff of the LRS was 2.2 to 2.5 times that of the FTS and soil loss was 2.7 to 3.1 times larger than that in the FTS (Table 2). The CRS was able to hold all of the rainfall in furrows during the 50 mm $h^{-1}$ treatment, thus total runoff and soil loss were nearly zero for the low rainfall treatment. For the moderate and high rainfall, total runoff and soil loss for the CRS depended upon whether the ridges were breached or not with minimal runoff and soil loss prior to failure and excessive losses after failure (Table 2).

The runoff rate after contour failure was 2.1 times larger than that in the FTS but total runoff was about equal. The soil loss rate was 14.4 times larger for the CRS after failure than in the FTS in the 75 mm $h^{-1}$ treatment, however, the total soil loss rate was only 5.9 times higher. In comparison, the CRS after failure had 3 times lower runoff but 1.9 times higher soil loss than the LRS. In the 100 mm $h^{-1}$ treatment, the total runoff after contour failure was approximately the same as that in the FTS but 2.5 times smaller than that in the LRS. In contrasts, total soil loss was 1.8 times higher for the CRS after failure than for the FTS but still 1.2 times lower than for the LRS.

### 3.3. Flow velocity and shear stress in the FTS and LRS

Results for mean flow velocity and shear stress in the FTS and LRS based on Eqs. (2) and (3) are shown in Fig. 7. Among the three rainfall intensities, rill flow velocities in the LRS were 1.03 to 2.29 times larger than sheet flow velocities in the FTS. Shear stress for the LRS was also around twice that of the FTS.

In the FTS, flow velocity in the 75 and 100 mm $h^{-1}$ treatments increased by 48% and 85% compared with that in the 50 mm $h^{-1}$ treatment. Shear stress in the FTS also increased when rainfall intensity increased. In the LRS, mean flow velocity remained constant, ranging from 18.1 to 20.1 cm $s^{-1}$ while shear stress slightly increased with rainfall intensity.

## 4. Discussion

### 4.1. Comparisons of runoff and soil loss in different tillage systems

Soil loss differences in different tillage systems were associated with the erosion processes. The dominant erosion process in the FTS was sheet erosion involving raindrop splash and shallow flow erosion (Fig. 3c). While in the LRS, the erosion process quickly evolved from splash and sheet erosion to a convergent flow erosion processes within furrow which dramatically increased the soil loss (Fig. 3 and Table 2). In the LRS, soil particles were first detached by raindrop splash on ridge tops and sidewalls. As run time progressed, a soil seal/crust formed on the surface of the ridge body which prevented further soil detachment to some extent. The seal increased runoff from ridge tops and side-slopes into furrows. In the furrow bottom and ridge side-slopes there were several rill headcuts and sidewall collapses formed by convergence of upstream runoff in furrows (Fig. 3a). In addition, ridge side-slopes exhibited rills which revealed the convergence of runoff from ridge tops along ridge side-slopes (Liu et al., 2014a, 2016). Rill formation enhanced the erosive hydraulic forces and sediment transport ability by converging and capturing runoff on the ridge side-slopes which increased the soil loss (Li et al., 2016; Shen et al., 2016).

The general consensus is that contour ridges can increase water infiltration before breaching (USDA-ARS, 2008, 2013; Liu et al., 2015). However, once the water storage capacity of the furrows is exceeded such that ridges are over-topped, water stored in the furrows concentrates the runoff at the lowest or weakest point along the ridge body thereby creating a failure point. At each failure location, over-topping created a headcut at the lower side of ridges (Fig. 8) that advanced upslope across the ridge, i.e. backwards erosion, until the ridge was breached. Water flowing through the breach went downslope to the next furrow and the increased water volume caused a subsequent failure in the downslope ridge. These failures cascaded downslope

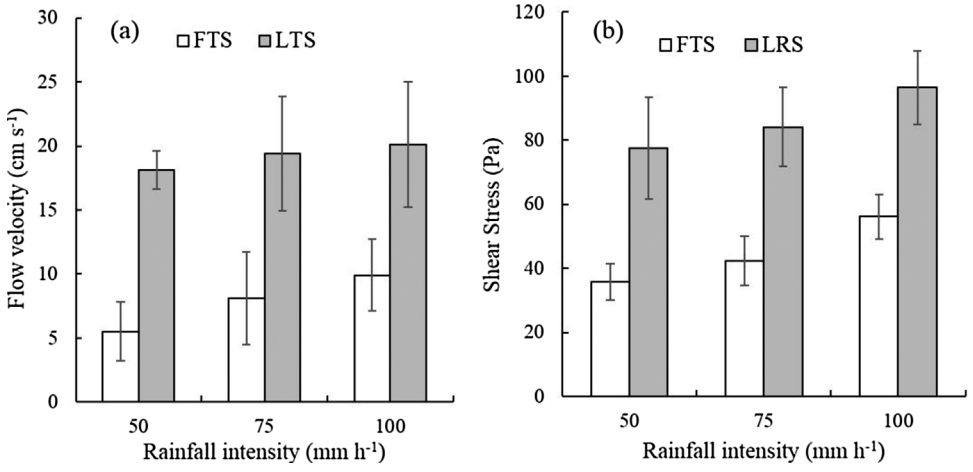


**Fig. 7.** Mean flow velocity and shear stress of sheet flow in the FTS and rill flow in the LRS.

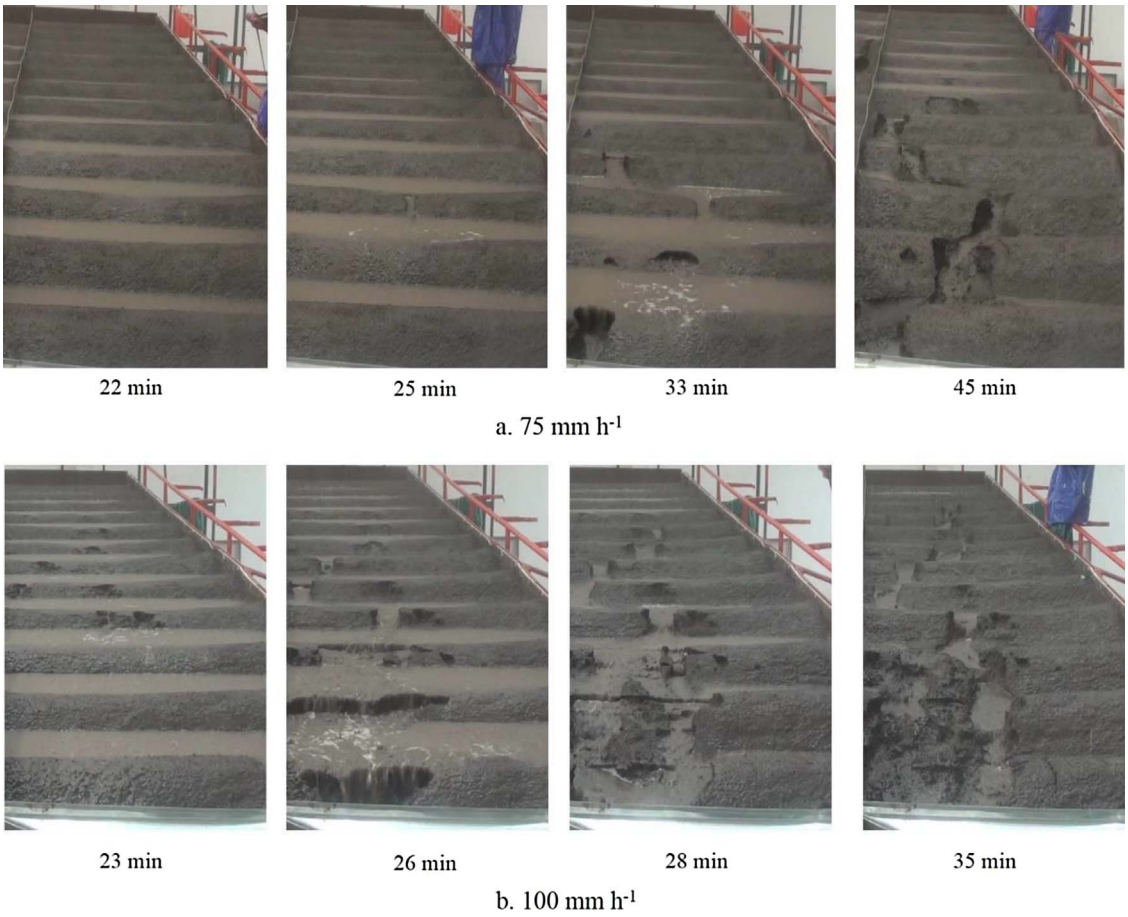


**Fig. 8.** Contour ridge failures by breaching of ridges with time for the 75 and 100 mm $h^{-1}$ treatments.

(Fig. 8) until runoff was observed at the outlet (Fig. 4) and resulted in ephemeral gully formation. The runoff rate peak value and occurrence time was mainly related to the spatial and temporal distribution of contour ridge breaching in this study (Fig. 8a and b).

In the CRS, changes in the sediment detachment and erosion processes separated the time series into two stages: before and after ridge failure. Before ridge failure, soil particles detached by raindrop splash produced surface sealing similar to that observed in the LRS. Sheet flow off the ridge top increased with time but the soil erosion from the ridge was trapped in the furrows with little to no overall soil losses. After overtopping of ridges occurred, the soil erosion processes changed to convergent flow erosion processes and mass failure of the ridge sidewalls. Soil particles and aggregates on the top surface of ridges were detached by the convergent overflow as breaches in the ridges rapidly occurred (Fig. 8a, 25 min in 75 mm $h^{-1}$ treatment). Within a brief time, breaches became connected to form an ephemeral gully through the contour ridges along the hillslope. After ephemeral gullies developed on the slope as a result of runoff connectivity, headcut retreat processes dominated the soil erosion processes (Fig. 8a, 33 min in 75 mm $h^{-1}$ treatment). This process was obviously accelerated in the 100 mm $h^{-1}$ treatment; it only took about 6 min from the start of overtopping to an ephemeral gully formed on the slope (Fig. 8b, 23–28 min in 100 mm $h^{-1}$ treatment). As a result, contour ridges provided an abundant source of sediment for concentrated flow to detach and transport as the erosion processes changed from sheet to rill to ephemeral gully erosion. The result were extremely high soil loss rates and sediment concentrations from the CRS after failure (Table 2). Similar runoff and sediment peaks related to the contour ridge failure were also found by other researchers (Liu et al., 2014a, 2015), whereby peak soil loss rates after ridge failure were about 40 times larger than before ridge collapse. The ratio of peak sediment rate to the base sediment rate in this study ranged from 10 to 20, which is not as high as that reported by Liu et al. (2014a). This is related to the differences in rainfall intensity, soil erodibility, ridge geometry and experimental setup.

### 4.2. Rill formation in the LRS

The FTS was dominated by sheet erosion under all conditions tested (Fig. 3c). In the LRS, the dominant erosion process changed from sheet erosion to rill erosion at the bottom of longitudinal furrows (Fig. 3a). Disconnected rill headcuts were formed in the furrow bottom after concentrated runoff occurred. Subsequently, rill headcut retreat linked these disconnected rill headcuts to an integrated rill, accompanied with rill bed incision and sidewall collapse processes (Fig. 3a). Soil loss from rills and its contribution to total soil loss were obtained by monitoring the rill morphology changes, and the results showed that rill erosion occupied 55.2% to 65.8% of total soil loss in the LRS. This contribution percentage is a little smaller than that observed by Shen et al. (2016) on loessial soil with manual tillage performed at about 20 cm depth along the contour line. The contribution differences can be attributed to differences in soil characteristics, tillage practices, and topographic conditions as rill contributions vary over a large range of environmental conditions and monitoring methods (Govers and Poesen, 1988). Mean flow velocity and shear stress differences in the LRS and FTS illustrated the big differences in soil erosion (Table 2, Fig. 7). As flow velocity increased, soil particle detachment and sediment transport ability dramatically increased, which resulted in more soil loss monitored at the outlet (Li et al., 2016).

**Table 3**
Water storage volume of contour ridge system under different rainfall intensities.

| Rainfall intensity (mm $h^{-1}$) | Time of ridge failure (min) | Water storage (mm) |
|---|---|---|
| 50 | – | 37.5 |
| 75 | 29.5 ± 0.7 | 36.9 ± 0.9 |
| 100 | 22.0 ± 0.8 | 36.7 ± 1.4 |

### 4.3. Contour ridge stability and ephemeral gully formation in the CRS

A critical parameter for reflecting contour ridge stability is the water storage capacity of the furrows during rainfall, which was calculated and summarized in Table 3. In the 50 mm $h^{-1}$ treatment, 37.5 mm rainwater was infiltrated or impounded by contour ridges during the 45 min rainfall duration. In the 75 and 100 mm $h^{-1}$ treatments, ridge failure occurred at separate times (7.5 min difference on average) but the water storage volume at the time of failure was nearly the same, 36.9 and 36.7 mm in Table 3. Although ridge failure occurred at different times for the different rainfall intensity treatments, the water volume intercepted (including infiltration and impoundment) were nearly the same. Thus the ridge geometry controlled the water-storage capacity which was constant as the rainfall intensity varied. This result revealed the significance of ridge geometry on erosion in the CRS (Liu et al., 2014b, 2015; USDA-ARS, 2013). As generally recommended on small field slopes, it may be useful to design the ridge heights according to the expected rainfall intensity and duration in the specific region to prevent contour ridge failure and decrease the risk of soil loss hazard (Liu et al., 2014a).

Given the propensity of contour ridges to fail by overtopping under large (> 50 mm $h^{-1}$) rainfall events, the microtopography and ability to engineer ridges exactly on the contour become critical factors in their ability to control runoff and erosion. Micro-depressions in the ridges will provide break-points for failure and the initiation of ephemeral gullies in the CRS (USDA-ARS, 2008; An et al., 2015). A field investigation conducted in Zaka District in southern Zimbabwe showed that contour ridges, which were implemented as a cure for rill erosion, have instead become a cause of rill and ephemeral gully erosion (Hagmann, 1996) and in many cases, contour ridges are major contributors to accelerated ephemeral gully erosion resulting from the concentration of water flow through ridge failures. This phenomenon is also common in the North China Plain (Liu et al., 2014a, 2014b) and Mollisol region of Northeast China (Meng and Li, 2009; Zhang, 2016) because of ridge microtopography changing the CRS. When rainwater or snowmelt runoff occurs, sediment detached from the ridge body by raindrop or surface runoff is transported to the furrows and deposited there. This erosion/deposition process increases the baseline height of furrows, thereby reducing the storage capacity and making subsequent concentrated flows easier to overtop ridges. The result of overtopping is severe ephemeral gully erosion that causes dramatic amounts of soil loss. A field survey in a small catchment in a typical Mollisol area showed that the density of ephemeral gullies initiated by concentrated flow overtopping in depressional areas reached 0.74 km $km^{-2}$ (Su et al., 2012). The results of this study emphasized the importance of this process and the need to manage ridge geometry for determining the water storage capacity. Increases in ridge height and spacing, accompanied with ridge quality management, are highly recommended. More research should be done on contour failure induced ephemeral gully erosion to better understand and model this process in ridge tillage systems of the Mollisol region.

### 4.4. Limitations of simulation experimental study

Although laboratory based rainfall simulations are common in erosion studies due to their efficiency and ability to control the governing variables for a wide range of hydrologic, pedologic, and topographic conditions, there are still limitations for studying tillage systems such as the plot size not fully representing real field conditions. For this study, runoff was forced to accumulate within furrows because it could not drain laterally due to the side walls of the soil pan. Thus over-topping of ridges would occur once the furrow storage was exceeded. In a real field, ridges are not perfectly on the contour; as such, overland flow may drain off along furrows to field edges or converge to depressions within fields. Thus the breaching effect may occur at different times and rainfall intensities compared with the results observed in this study. It can be concluded that under ideal field conditions when ridges are perfectly mounded on contour lines, 37 mm is a good estimate for water storage capacity of the ridge geometries used in this study and the breaching dynamics of ridges would occur as observed in this study. However, if ridges are off the contour, water storage capacity may not be exceed due to drainage off rows or may be exceeded sooner due to depressional convergence.

### 4.5. Tillage practices in the Mollisol region of Northeast China

There is a long-lasting discussion on which ridge tillage method (longitudinal ridge or contour ridge tillage method) is better on the gentle slope farmland to control the soil loss (Shen et al., 2005). According to the result of this experiment and long term tillage practice experiences, when rainfall intensity is small, runoff and soil loss will not occur on either LRS or CRS system and all rainwater is infiltrated. When rainfall intensity is larger than the infiltration rate, surface runoff will occur in the LRS and convergent flow along LRS furrows cause severe soil loss although the overall slope gradient is small. Changing LRS to CRS has shown positive effects on runoff and soil loss control (Chen et al., 2008; Liu et al., 2011; Zhang et al., 2011). However, severe ephemeral gully has been observed on such farmlands as a result of CRS ridge failures which is forcing some farmers to reconsider this choice.

Farmers in this region are more willing to use LRS for several reasons. First and foremost, it is convenient and the traditional method of tillage and as long as the rainfall intensity is low it does not cause severe soil erosion. Second, although soil erosion is serious in big storms, the crops on the ridge body are generally not damaged such that the effect of the soil loss is not readily identifiable in the crop yield (Fig. 1a; Shen et al., 2005). Third, contour ridges are not good for drainage which is considered by farmers to be a priority for early access to field following snowmelt. It is often observed that the ridge body when placed on contours is easily saturated when water accumulates in the furrows and can result in seepage at the base of downslope ridges (Fig. 1b). This process negatively affects ridge stability and can induce more soil loss when ridges breach (Liu et al., 2016). Furthermore, the CRS cannot follow contour line strictly in practice, thus, small row degree may cause negative impacts on soil erosion control (Liu et al., 2014a, 2014b). Modified ridge methods may be able to retain the rainwater and snow melt water, reduce runoff and soil loss, increase crop water use efficiency, and produce economic benefits (Dagg and Macartney, 1968; Hagmann, 1996) such as tied ridge, furrow dikes, basin tillage, furrow blocking, or reservoir tillage (Jones and Clark, 1987; Shen et al., 2005; Temesgen et al., 2009; Araya and Stroosnijder, 2010). These measures provide more space in furrows which is beneficial for increasing water storage capacity and reducing the likelihood of contour ridge failure. Other practices such as double furrows with raised beds (Gammoh, 2011), and broad furrows (Omer and Elamin, 1997) should also be considered.

This study showed low runoff and soil loss rates in the FTS (Table 2), thus, flat slope tillage system is highly recommended on the gentle farmland compared to the ridge tillage systems for soil erosion control. Better residue management may increase infiltration in conservation tillage systems such as reduced-tillage or no tillage with either CRS or FTS is also recommended (Stevens et al., 2009; Chen et al., 2011). However, there is a concern for the impact of these practices on soil temperatures (Wall and Stobbe, 1984; Dahiya et al., 2007) in cold

regions at high latitude. Another problem of CRS and no-till combinations is that ridges may slowly disappear when not frequently rebuilt over time (e.g., through erosion of ridge tops and side slopes and sedimentation of furrows). Strip tillage conserves water and soil with a higher soil temperature and is widely applied in high latitude areas, e.g., Iowa, Indiana, Ohio, and Vancouver, etc. (Griffith et al., 1973; Hares and Novak, 1992; Licht and Al-Kaisi, 2005), which may also be an appropriate choice for the Mollisol region of Northeast China. Contour ridges are effective for erosion control when no contour failure occurs. Thus it can be an effective way to provide good seed bed environment and reduce soil erosion if properly designed and managed in the Mollisol region. Based on the finding that water storage capacity did not vary with rainfall intensity above 50 mm $h^{-1}$, increasing ridge height and space between ridges could reduce erosion as it would considerably lower the likelihood of ridge failures at high rainfall intensities and long durations. Future work testing contour ridge stability is still needed.

## 5. Conclusions

Simulated rainfall-erosion experiments that focused on the comparison of runoff and soil loss in the LRS, CRS and FTS were conducted under three rainfall intensities (50, 75 and 100 mm $h^{-1}$) and slope gradient of 5°. The ridge geometry was designed according to field measurements and tillage machine sizes used in the farmlands of Northeast China. The results showed that: 1) runoff and soil loss in the LRS were larger than those in the FTS due to the erosion patterns changing from sheet to rill erosion as a result of increased convergent flow velocity and shear stress; 2) water storage capacity of contour ridges remained constant as rainfall intensity increased; 3) contour ridge failure as a result of storage capacity of furrows being exceeded occurred in the 75 and 100 mm $h^{-1}$ treatments of the CRS; 4) overtopping of contour ridges changed the runoff and soil loss from sheet and rill erosion to ephemeral gully erosion processes; 5) breached ridges and the resulting ephemeral gullies provided an excessive source of sediment; and 6) soil losses observed in both ridge tillage systems were attributed to rill or ephemeral gully formation which should be given more attention in future assessments. This study recommends use of flat tillage in large storm and long slope conditions to control soil erosion in the Mollisol region of Northeast China. Modifications of the CRS, e.g., increasing ridge height and space between ridges, or enlarging the furrow space using dikes, to increase the water storage capacity and retain the rainwater as well as snowmelt water, may also effectively reduce soil erosion.

## Acknowledgments

This study was supported by the Strategical International Collaborative Special Project of Scientific and Technological Innovation for the National Key Development Plan (2016YFE0202900), National Natural Science Foundation of China (No. 41571263), and China Scholarship Council funds. The authors would like to thank Dr. Seth M. Dabney and anonymous reviewers for their constructive suggestions.

## References

An, J., Zheng, F.L., Lu, J., Li, G.F., 2012. Investigating the role of raindrop impact on hydrodynamic mechanism of soil erosion under simulated rainfall conditions. Soil Sci. 177 (8), 517–526.
An, J., Liu, Q.J., Wu, Y.Z., 2015. Optimization of the contour ridge system for controlling nitrogen and phosphorus losses under seepage condition. Soil Use Manage. 31 (1), 89–97.
Araya, A., Stroosnijder, L., 2010. Effects of tied ridges and mulch on barley (Hordeum vulgare) rainwater use efficiency and production in Northern Ethiopia. Agric. Water Manage. 97 (6), 841–847.
Arnhold, S., Ruidisch, M., Bartsch, S., Shope, C.L., Huwe, B., 2013. Simulation of runoff patterns and soil erosion on mountainous farmland with and without plastic-covered ridge-furrow cultivation in South Korea. Trans. ASABE 56 (2), 667–679.
Benjamin, J.G., Blaylock, A.D., Brown, H.J., Cruse, R.M., 1990. Ridge tillage effects on simulated water and heat transport. Soil Tillage Res. 18 (2), 167–180.
Chen, X., Cai, Q.G., Wang, X.Q., 2008. Suitability of soil and water conservation measures on sloping farmland in typical black soil region of Northeast China. Sci. Soil Water Conserv. 6 (5), 44–49 (in Chinese).
Chen, Y., Liu, S., Li, H., Li, X.F., Song, C.Y., Cruse, R.M., Zhang, X.Y., 2011. Effects of conservation tillage on corn and soybean yield in the humid continental climate region of Northeast China. Soil Tillage Res. 115, 56–61.
Dagg, M., Macartney, J.C., 1968. The agronomic efficiency of the NIAE mechanized tied ridge system of cultivation. Exp. Agric. 4 (4), 279–294.
Dahiya, R., Ingwersen, J., Streck, T., 2007. The effect of mulching and tillage on the water and temperature regimes of a loess soil: experimental findings and modeling. Soil Tillage Res. 96 (1), 52–63.
Fausey, N.R., 1990. Experience with ridge-till on slowly permeable soils in Ohio. Soil Tillage Res. 18 (2–3), 195–205.
Free, G.R., 1956. Investigations of tillage for soil and water conservation I. A comparison of crop yields for contour vs. up and downslope tillage. Soil Sci. Soc. Am. J. 20 (3), 427–429.
Gürsoy, S., Sessiz, A., Karademir, E., Karademir, Ç., Kolay, B., Urğun, M., Malhi, S.S., 2012. Effects of ridge and conventional tillage systems on soil properties and cotton growth. Int. J. Plant Prod. 5 (3), 227–236.
Gammoh, I.A., 2011. Double furrow with raised bed—a new improved mechanized water-harvesting technique for large-scale rehabilitation of arid rain-fed areas. Soil Tillage Res. 113 (1), 61–69.
Gebreegziabher, T., Nyssen, J., Govaerts, B., Getnet, F., Behailu, M., Haile, M., Deckers, J., 2009. Contour furrows for in situ soil and water conservation, Tigray, Northern Ethiopia. Soil Tillage Res. 103 (2), 257–264.
Govers, G., Poesen, J., 1988. Assessment of the interrill and rill contributions to total soil loss from an upland field plot. Geomorphology 1 (4), 343–354.
Griffith, D.R., Mannering, J.V., Galloway, H.M., Parsons, S.D., Richey, C.B., 1973. Effect of eight tillage-planting systems on soil temperature, percent stand, plant growth, and yield of corn on five Indiana soils. Agron. J. 65 (2), 321–326.
Hagmann, J., 1996. Contour ridges: cure for, or cause of, rill erosion? Land Degrad. Dev 7, 145–160.
Hares, M.A., Novak, M.D., 1992. Simulation of surface energy balance and soil temperature under strip tillage: II. Field test. Soil Sci. Soc. Am. J. 56 (1), 29–36.
Hatfield, J.L., Allmaras, R.R., Rehm, G.W., Lowery, B., 1998. Ridge tillage for corn and soybean production: environmental quality impacts. Soil Tillage Res. 48 (3), 145–154.
He, J., Li, H.W., Kuhn, N.J., Wang, Q.J., Zhang, X.M., 2010. Effect of ridge tillage, no-tillage, and conventional tillage on soil temperature, water use, and crop performance in cold and semi-arid areas in Northeast China. Soil Res. 48 (8), 737–744.
Jaynes, D.B., Swan, J.B., 1999. Solute movement in uncropped ridge-tilled soil under natural rainfall. Soil Sci. Soc. Am. J. 63 (2), 264–269.
Jones, O.R., Clark, R.N., 1987. Effects of furrow dikes on water conservation and dryland crop yields. Soil Sci. Soc. Am. J. 51 (5), 1307–1314.
Lal, R., 1990. Ridge-tillage. Soil Tillage Res. 18 (2–3), 107–111.
Li, G.F., Zheng, F.L., Lu, J., Xu, X.M., Hu, W., Han, Y., 2016. Inflow rate impact on hillslope erosion processes and flow hydrodynamics. Soil Sci. Soc. Am. J. 80 (3), 711–719.
Licht, M.A., Al-Kaisi, M., 2005. Strip-tillage effect on seedbed soil temperature and other soil physical properties. Soil Tillage Res. 80 (1), 233–249.
Liu, X., Yan, B., 2009. Soil and water loss and food security in Northeast black soil region. Chin. Soil Water Conserv. 1, 17–19 (in Chinese).
Liu, X., Zhang, S., Zhang, X., Ding, G., Cruse, R.M., 2011. Soil erosion control practices in Northeast China: a mini-review. Soil Tillage Res. 117, 44–48.
Liu, H., Zhang, T., Liu, B., Liu, G., Wilson, G.V., 2013. Effects of gully erosion and gully filling on soil depth and crop production in the black soil region, northeast China. Environ. Earth Sci. 68 (6), 1723–1732.
Liu, Q.J., Zhang, H.Y., An, J., Wu, Y.Z., 2014a. Soil erosion processes on row sideslopes within contour ridging systems. Catena 115, 11–18.
Liu, Q.J., Shi, Z.H., Yu, X.X., Zhang, H.Y., 2014b. Influence of microtopography, ridge geometry and rainfall intensity on soil erosion induced by contouring failure. Soil Tillage Res. 136, 1–8.
Liu, Q.J., An, J., Wang, L.Z., Wu, Y.Z., Zhang, H.Y., 2015. Influence of ridge height, row grade, and field slope on soil erosion in contour ridging systems under seepage conditions. Soil Tillage Res. 147, 50–59.
Liu, L., Liu, Q.J., Yu, X.X., 2016. The influences of row grade, ridge height and field slope on the seepage hydraulics of row sideslopes in contour ridge systems. Catena 147, 686–694.
Lu, J., Zheng, F.L., Li, G.F., Bian, F., An, J., 2016. The effects of raindrop impact and runoff detachment on hillslope soil erosion and soil aggregate loss in the Mollisol region of Northeast China. Soil Tillage Res. 161, 79–85.
Meng, L.Q., Li, Y., 2009. The mechanism of gully development on sloping farmland in black soil area, Northeast China. J. Soil Water Conserv. 23 (1), 7–11 (in Chinese).
Mert, M., Aslan, E., Akişcan, Y., Çalişkan, M.E., 2006. Response of cotton (Gossypium hirsutum L.) to different tillage systems and intra-row spacing. Soil Tillage Res. 85 (1), 221–228.
Nearing, M.A., Bradford, J.M., Parker, S.C., 1991. Soil detachment by shallow flow at low slopes. Soil Sci. Soc. Am. J. 55, 339–344.
Omer, M.A., Elamin, E.M., 1997. Effect of tillage and contour diking on sorghum establishment and yield on sandy clay soil in Sudan. Soil Tillage Res. 43 (3–4), 229–240.
Reeder, R.C., 1990. Extension programs and farmer experiences with ridge tillage. Soil Tillage Res. 18 (2–3), 283–293.
Shen, C.P., Gong, Z.P., Wen, J.T., 2005. Comparison study on soil and water loss of cross ridge and longitudinal ridge. Bull. Soil Water Conserv. 25 (4), 48–49 (in Chinese).

Shen, H.O., Zheng, F.L., Wen, L.L., Han, Y., Hu, W., 2016. Impacts of rainfall intensity and slope gradient on rill erosion processes at loessial hillslope. Soil Tillage Res. 155, 429–436.
Stevens, C.J., Quinton, J.N., Bailey, A.P., Deasy, C., Silgram, M., Jackson, D.R., 2009. The effects of minimal tillage, contour cultivation and in-field vegetative barriers on soil erosion and phosphorus loss. Soil Tillage Res. 106 (1), 145–151.
Su, Z.L., Cui, M., Fan, H.M., 2012. Effect of shelterbelts distribution on ephemeral gully erosion in rolling-hilly black soil region of Northeast China. Res. Soil Water Conserv. 19 (3), 20–23 (in Chinese).
Temesgen, M., Hoogmoed, W.B., Rockstrom, J., Savenije, H.H.G., 2009. Conservation tillage implements and systems for smallholder farmers in semi-arid Ethiopia. Soil Tillage Res. 104, 185–191.
USDA-ARS, 2008. User's reference guide, Revised Universal Soil Loss Equation Version 2. http://www.ars.usda.gov/sp2UserFiles/Place/64080510/RUSLE/RUSLE2_User_Ref_Guide.pdf.
USDA-ARS, 2013. Science documentation, Revised Universal Soil Loss Equation Version 2. https://www.ars.usda.gov/ARSUserFiles/60600505/RUSLE/RUSLE2_Science_Doc.pdf.
Wall, D.A., Stobbe, E.H., 1984. The effect of tillage on soil temperature and corn (Zea mays L.) growth in Manitoba. Can. J. Plant Sci. 64 (1), 59–67.
Wischmeier, W.H., Smith, D.D., 1978. Predicting Rainfall Erosion Losses: A Guide to Conservation Planning. U.S. Department of Agriculture, Agric. Handb. pp. 537.
Yang, W., Zheng, F., Han, Y., Wang, Z., Yi, Y., Feng, Z., 2016. Investigating spatial distribution of soil quality index and its impacts on corn yield in a cultivated catchment of the Chinese Mollisol region. Soil Sci. Soc. Am. J. 80 (2), 317–327.
Zhang, Y., Wu, Y., Liu, B., Zheng, Q., Yin, J., 2007. Characteristics and factors controlling the development of ephemeral gullies in cultivated catchments of black soil region, Northeast China. Soil Tillage Res. 96 (1), 28–41.
Zhang, S., Zhang, X., Huffman, T., Liu, X., Yang, J., 2011. Influence of topography and land management on soil nutrients variability in Northeast China. Nutr. Cycl. Agroecosys. 89 (3), 427–438.
Zhang, T.Y., 2016. Measurement and calibration of ephemeral gully depth in ridge tillage croplands. Sci. Soil Water Conserv. 14 (5), 138–144 (in Chinese).